Local Forcing of a Nonlinear Surface Reaction: CO Oxidation on Pt(100)

Daniel Bilbao, Noah McMillan, and Jochen Lauterbach
Center for Catalytic Science and Technology, Dept. of Chemical Engineering, University of Delaware, Newark, DE 19716

Christopher M. Snively
Depts. of Chemical Engineering and Materials Science, University of Delaware, Newark, DE 19716

DOI 10.1002/aic.11655
Published online October 29, 2008 in Wiley InterScience (www.interscience.wiley.com).

A novel spatiotemporal perturbation method for nonlinear surface reactions is reported, thus allowing the creation of new spatially localized structures. Forcing was achieved by dosing reactant gases through a capillary positioned near the catalyst surface, providing control over the local surface coverage and reaction rate. The emergence of localized concentration patterns and oscillations in an otherwise stable system is attributed to a local modification of the catalytic properties of the surface due to external forcing. Based on the spatial orientation, the temporal and thermal stability of the modified surface, as well as the affinity of CO toward the perturbed surface, subsurface O is proposed as a possible source of the observed localized patterning and surface memory effect. © 2008 American Institute of Chemical Engineers *AIChE J,* 55: 172–179, 2009

Keywords: CO oxidation, pattern formation, external forcing

Introduction

Forcing of nonlinear systems is a subject of rapidly increasing interest, because of the potential to not only generate but also control and exploit complex dynamic behavior. Forcing of chemical systems has been demonstrated by a variety of methods in both homogeneous and heterogeneous systems.[1–5]

In catalytic systems that exhibit rich spatiotemporal complexity, such as CO oxidation on platinum, external global temporal forcing was shown to lead to different oscillations and spatiotemporal patterns than those which occur in unforced systems.[1] Examples include the bounding of chemical waves on micropatterned catalysts,[6] the creation and destruction of chemical waves by local perturbation of the catalyst temperature,[7] and the use of IR thermography to observe changes in the rate of CO oxidation for local perturbations by bursts of CO released near a catalyst surface.[8,9] Our experiments demonstrate the ability to locally perturb the gas-phase composition near a heterogeneous catalyst surface with reactants such as O_2, H_2, and CO to induce unique spatiotemporal behavior. The resulting spatially localized structures have not previously been observed in the unforced system under similar conditions.

Spatiotemporal pattern formation on single crystal surfaces occurs due to nonlinear feedback. In vacuum, such nonlinear phenomena are isothermal and driven by the kinetics of surface processes. Oscillations and pattern formation during CO oxidation on Pt(100) were explained by the adsorbate-induced surface reconstruction, where the surface switches between a highly reactive oxygen-covered state a less reactive CO-poisoned state.[10–12] At low coverages, the surface atoms of Pt(100) rearrange into a quasi-hexagonal (hex) reconstruction.[13,14] On this phase, the adsorption probability of O_2 is around 10^{-3}, as compared to almost one for CO.[14–17] Above a critical coverage of CO and/or oxygen on the hex surface, the reconstruction is lifted to a 1×1 surface arrangement,[18–20] which causes an increase in the adsorption

Correspondence concerning this article should be addressed to J. Lauterbach at lauterba@udel.edu.

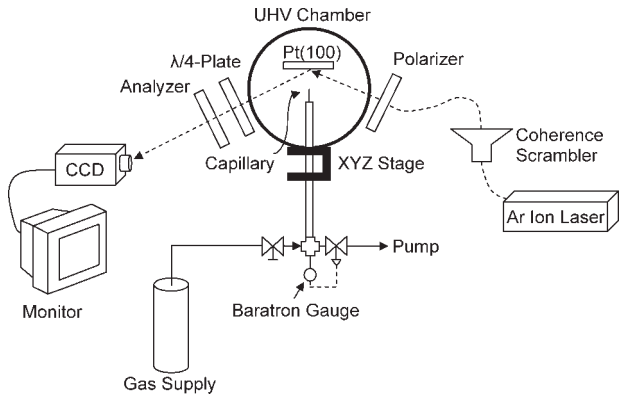

Figure 1. Experimental setup including imaging ellipsometer (EMSI) and local gas dosing equipment used to externally perturb the surface reaction.

EMSI provides a spatially resolved, greyscale image, where the contrast of the image is due to the presence of different adsorbates. The local gas doser consists of a capillary fastened to a ¼'' tube, all of which is mounted on an xyz stage. The doser is fed with reactant through a differentially pumped inlet. A pulse valve located at the end of the capillary allows for control over the frequency of the applied perturbation.

probability of O_2 to approximately 0.1.[14–16] Coupling of this feedback mechanism with surface diffusion of adsorbed molecules gives rise to self-sustained pattern formation.[21,22]

Experimental

All experiments were conducted on a Pt(100) single crystal catalyst under continuous flow conditions within a stainless steel UHV chamber containing reactants at constant pressure. The chamber was equipped with an ion gun for sample cleaning and a quadrupole mass spectrometer (Hiden HAL-201) used for monitoring reaction products. The sample was mounted in the chamber on an x-y-z manipulator by means of two Ta wires spot welded to the back of the sample. The sample could be heated resistively by passing current through the Ta wires, and a type-K thermocouple, also spot welded to the back of the sample, was used to monitor sample temperature. Prior to experiments, a clean surface was prepared with repeated cycles of annealing to 1,200 K, Ar ion sputtering under 0.013 Pa Ar, and oxidation at 950 K and 1.3×10^{-4} Pa O_2. The catalyst surface was observed continuously using ellipsomicroscopy for surface imaging (EMSI), a real-time imaging technique sensitive to the presence of different adsorbates.[23] Figure 1 outlines the components of the ellipsomicroscope. A fiber optic was used to direct light emitted from a 5 W Ar ion laser toward the sample surface. Before impinging on the surface, the light was passed through a Glan-Thompson polarizer to linearly polarize the incident light. Upon reflection from the surface, the now elliptically polarized light was passed through a λ/4-plate returning the light to a linear polarization state. The linearly polarized light was then analyzed by a second polarizer before reaching the CCD camera. The instrument was calibrated to the null position, designated by the minimum in signal intensity, while the surface was O-covered. Adsorption of CO to the surface then locally altered the polarization state of the reflected light such that it was no longer compensated for by the optics, resulting in contrast in the final image. For these studies, CO-covered regions of the surface appear darker relative to areas of adsorbed oxygen.

External forcing of the surface reaction was achieved by locally dosing reactants onto the catalytic surface through a capillary having a 30 μm inside diameter (Figure 1). The capillary was mounted on an x-y-z translational stage and connected to a pressure controlled, differentially pumped gas inlet allowing for control over the intensity of the perturbation applied to the surface. A pulse valve located near the end of the capillary was used to regulate the forcing frequency.

In order to better understand the effects of forcing using the local gas dosing technique, it was necessary to characterize the relative flux of molecules within the molecular stream produced by the capillary. To accomplish this, the stream was locally sampled with a mass spectrometer using the apparatus illustrated in Figure 2. The system consisted of two adjacent vacuum chambers connected through a 10 μm laser-drilled orifice. The first chamber housed the local gas dosing equipment discussed previously. On the opposite side of the orifice, a second chamber included a mass spectrometer (SRS RGA300) used to measure the number of molecules from the stream which passed through the orifice into the second chamber. Helium was used as the dosing gas and was maintained at a pressure of 120 Pa upstream of the capillary to simulate the conditions of a typical forcing experiment. By scanning the local gas doser in the plane perpendicular to the orifice, the variation in the mass spectrometer signal provided a spatially resolved measurement of the relative gas fluxes experienced by the catalytic surface during local gas dosing.

Results and Discussion

Local O_2 dosing

For the unforced or globally perturbed CO oxidation system, oscillations and patterns typically develop over the

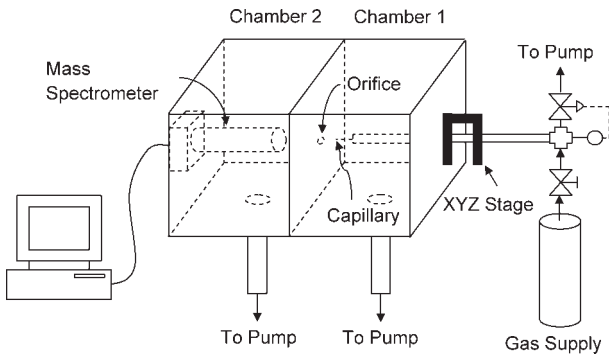

Figure 2. System used to locally sample molecular stream emitted from capillary using a mass spectrometer.

A 10 μm orifice separates the local doser, housed in chamber 1, from the mass spectrometer in the second chamber. Scanning the doser in the xy plane perpendicular to the orifice provided a spatially resolved representation of the relative gas fluxes experienced by the surface during a forcing experiment.

entire catalytic surface in response to particular global conditions. Utilizing local O_2 perturbations, however, discrete surface regions were promoted from a monostable, low-reactive state into a state of locally confined, self-sustained oscillations. A uniform surface was initially prepared by saturating the surface with CO. The reaction conditions were then set to $p_{O2} = 0.053$ Pa, with $p_{CO}/p_{O2} = 0.025$, and T = 510 K to maintain a uniform, CO-poisoned state. A pulse of O_2 from the microdoser was directed at the surface, and the high-local concentration of O_2 resulted in the formation of an oxygen island that expanded into the CO adlayer, as shown in Figure 3a, where the light grey regions correspond to oxygen covered surfaces and the dark grey denotes CO-covered areas. Reaction with the surrounding adsorbed CO removed the oxygen island from the surface, restoring the surface to the original, CO-covered state. Approximately 30 s after the disappearance of the induced oxygen island, however, an oxygen front spontaneously appeared (Figure 3b). This front spread across the area previously affected by the doser and was removed by a CO front, until the oxygen covered area had virtually disappeared again (Figure 3d). This sequence repeated for periods lasting up to 15 min, demonstrating the induction of self-sustained and locally constrained oscillations in an area surrounded by a monostable, CO-poisoned surface without an ongoing external stimulus.

The oscillations were always spatially restricted to the surface region initially affected by the microdoser, with the majority of oscillations occurring approximately every 50 s. The period of oscillation varied irregularly from 35 to 120 s for global conditions ranging from $p_{CO}/p_{O2} = 0.025$ at the onset of self-sustained oscillations, to $p_{CO}/p_{O2} = 0.018$, where the surface verged on transition to a high-reactive, oxygen covered state. A decrease in CO concentration did, however,

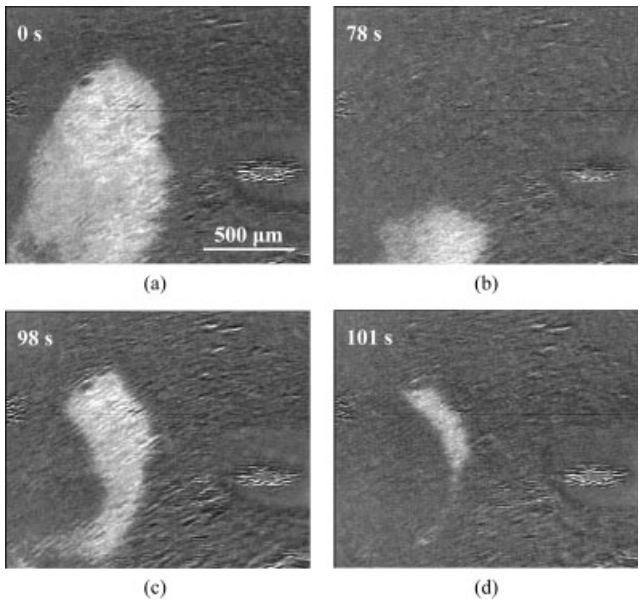

Figure 3. Initiation of locally confined oscillations.

(a) shows an oxygen island created on a monostable, CO-poisoned surface following an oxygen pulse from the microdoser, and (b)–(d) shows the subsequent appearance and reaction of a spontaneously formed oxygen front. T = 510 K, $p_{O2} = 0.053$ Pa, $p_{CO}/p_{O2} = 0.025$.

Table 1. Chemical Front Speed Observed During Spatially Restricted Oscillations

	Front Speed	
p_{CO}/p_{O2}	CO (μm/s)	O (μm/s)
0.025	10 ± 1	90 ± 10
0.018	2 ± 1	200 ± 40

slow observed CO front speeds from 10 to 2 μm/s, while the oxygen front speed approximately doubled from 90 to 200 μm/s. This trend, which is summarized in Table 1, is similar to that observed for chemical fronts in the unforced system for comparable pressures, and is attributed to the different mechanisms promoting CO and oxygen wave propagation.[24] The slower moving CO fronts are preceded by a low coverage, reconstructed hex fringe, upon which CO preferentially adsorbs due to a higher sticking probability. Adsorbed CO then diffuses and reacts with oxygen remaining on and ahead of the hex fringe to advance the CO front. In contrast, oxygen waves trail a fringe where the adsorbate coverages do not fall below the critical value necessary for the surface reconstruction to take place. Therefore, both O_2 and CO will readily adsorb on the 1×1 fringe, and, only in the presence of excess gas-phase O_2, can an autocatalytic oxygen wave form and propagate. Ultimately, this trend in front speed resulted in oscillations that became more relaxed in shape for decreased CO concentrations. Figure 4 includes space-time diagrams, which illustrate this behavior by plotting image intensity along the line segment AB (Figure 4a) as a function of time for gas-phase conditions of $p_{CO}/p_{O2} = 0.025$ (Figure 4b), and $p_{CO}/p_{O2} = 0.018$ (Figure 4c). At $p_{CO}/p_{O2} = 0.025$, the faster moving CO fronts were able to react away the adsorbed O island before another oscillation cycle began. Reduction of the CO concentration to $p_{CO}/p_{O2} = 0.018$ slowed the velocity of the propagating CO fronts, resulting in a slower decay to a low-reactive state followed by a fast transition to a high-reactive, oxygen covered surface before the O island could be completely reacted away.

Local H_2 dosing

Given the complexity of the seemingly "simple" bimolecular CO/O_2 system, the study of systems involving more than two reactant species is far from trivial. For example, the complex behavior of the catalytic CO oxidation reaction on Pt is further complicated by the introduction of H_2. For CO oxidation on Pt/SiO_2 catalysts, for example, a small amount of H_2 added to the gas phase caused a transition from sustained oscillatory behavior to a highly reactive steady state.[25] It was suggested that this behavior was the result of a nonuniform distribution of adsorbates on the catalyst surface. H_2 dissociatively adsorbs on Pt(100), lifting the reconstruction,[18,26] and was found to significantly modify the structure of the catalyst surface, pointing to the importance of H_2-induced defects on the Pt(100) surface.[26,27] Direct local dosing of H_2 onto the catalytic surface can assist in the elucidation of nonlinear phenomena in such complex nonlinear reaction systems.

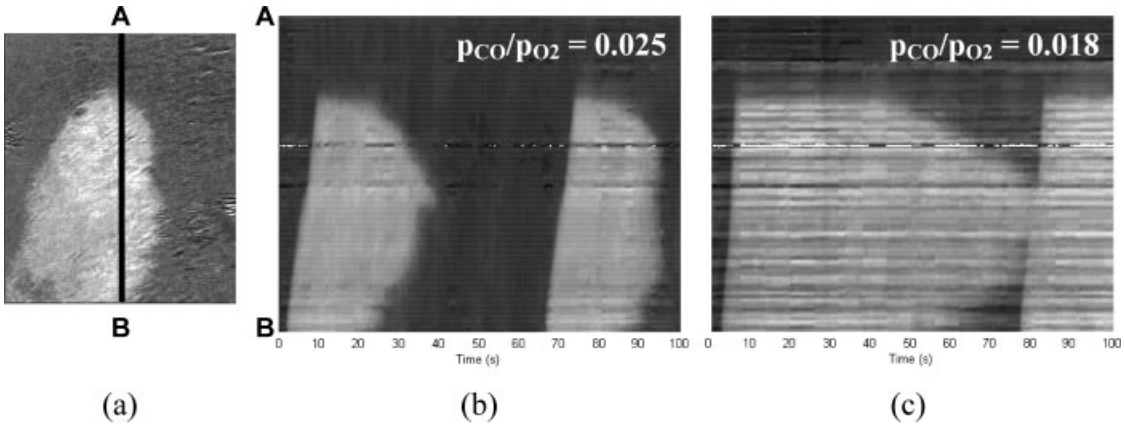

Figure 4. Space-time diagrams showing the influence of global CO concentration on the locally confined oscillations.

(b) and (c) plot the intensity over time along line segment AB (see (a)) for decreasing CO concentration. At $p_{CO}/p_{O2} = 0.025$, CO is able to completely react away the adsorbed oxygen island before the appearance of another oscillation. For $p_{CO}/p_{O2} = 0.018$, the decreased supply of CO to the reaction front slowed the propagation of the CO waves, resulting in a slower relaxation to the low-reactive state. Light grey regions correspond to oxygen covered regions and dark grey denotes CO covered areas. The length of segment AB in (a) is 1.1 mm. T = 510 K, $p_{O2} = 0.053$ Pa.

One novel result of these investigations is the creation of CO islands under reaction conditions via local H_2 dosing. Figure 5 shows an example of this process, where the sequence of numbers on the 20 s frame indicates the order in which the islands were created. The chamber was backfilled with O_2 and CO, with the doser positioned 500 μm from the catalyst surface. The catalyst surface was monostable and oxygen covered at the reaction conditions chosen. H_2 was then allowed to flow through the capillary, causing an area approximately 100 μm in diameter to be cleared of oxygen by reaction with hydrogen to form water. Both H_2 and water have low-energies of desorption, as compared to oxygen, such that coverage of these species is expected to be low at the temperatures of interest.[15,16,28,29] The local dosing of H_2 and its reaction to form water creates a nearly adsorbate-free area that can reconstruct to the hex phase. This area of the surface is then rapidly covered by CO, which adsorbs from the gas phase. This local CO poisoning is observed for CO concentrations as low as $p_{CO}/p_{O2} \sim 0.010$.

In Figure 5, H_2 was dosed onto the surface for approximately 2 s until the CO poisoning was observed. Following this, the doser was turned off and moved to another area of the surface where the process was repeated. The CO-poisoned areas are observed as dark circles in the EMSI images. As shown in the images, multiple CO islands were prepared by this method. When the H_2 doser was turned off, the surface, based on the behavior of the unperturbed reaction system, should have returned to the stable oxygen-covered state. In this example, all but one of the CO islands persisted on the surface, even growing for as long as 15 min, before being removed by a propagating oxygen wave initiated at the boundary of the island. The growth velocity of the islands, as shown in Figure 6, was between 0.1 to 2 μm/s, and increases with increasing CO concentration in the gas phase. The front velocities were a factor of 2–5 lower than in the case of an unperturbed reaction, however, in the unperturbed system, fronts were only observed for CO/O_2 ratios about 5 times higher than in the experiments reported here.

The growth of the CO islands on Pt(100) is consistent with the adsorbate-induced reconstruction model. The interior of the CO-poisoned islands is covered by a densely-packed CO adlayer, therefore oxygen cannot adsorb in high enough concentrations to generate wavefronts. On the edges of the island, the overall surface coverage is low due to the reaction of CO and oxygen, and the surface can reconstruct to the hex phase. As a result, adsorption on the edge of the CO island is dominated by CO, increasing the size of the island. The propagation of the CO islands is maintained by the reac-

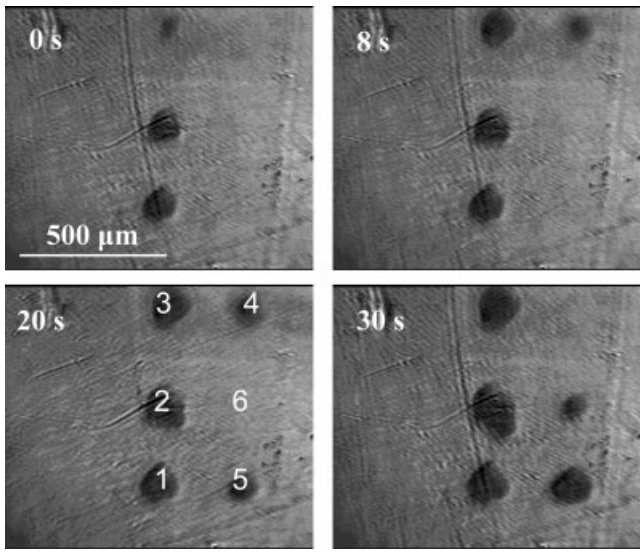

Figure 5. CO islands grow while surrounded by a monostable, chemisorbed oxygen phase.

Each island is prepared by dosing H_2 over the surface for ~2 s. After the appearance of the CO island, the H_2 perturbation is turned off and moved to a different location above the surface. T = 466 K, $p_{O2} = 0.013$ Pa, $p_{CO}/p_{O2} = 0.024$.

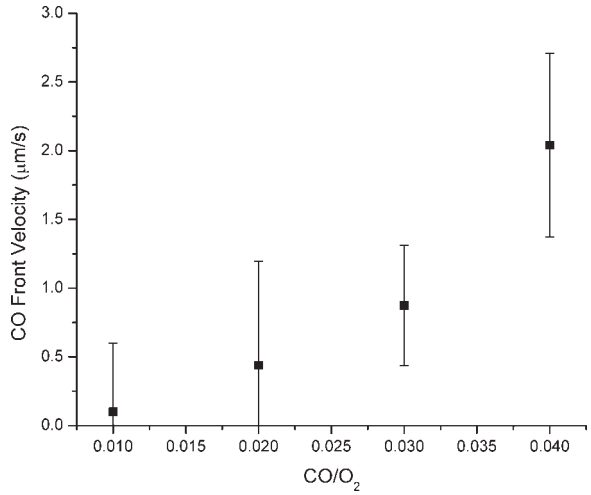

Figure 6. Propagation of CO islands as a function of gas phase composition under low p_{CO} conditions.

$p_{O2} = 0.013$ Pa, T = 473 K.

tion of CO with oxygen, the diffusion of CO across the catalyst surface, and the continuous adsorption of CO from the gas phase.

Surface modification due to external forcing

The appearance of spatially localized patterns on surface regions affected by external forcing implies that the catalytic properties of that particular region have been locally modified. These modifications facilitate patterning under conditions where such structures are not observed on unforced regions of the surface. Further evidence of local surface modification is shown in Figure 7, with the selective adsorption of CO to an O-covered surface following a local CO perturbation from the doser. Beginning with an oxygen covered surface maintained at 413 K with 0.013 Pa O_2, CO was locally dosed onto the surface to form an island of adsorbed CO surrounded by the O adlayer (Figure 7a). After 70 s, the local CO perturbation was removed and the affected surface region recovered to an O-covered state as shown in Figure 7b. At this point, 0.0013 Pa of CO was added to the gas phase to induce a transition from the O-covered state to a CO-poisoned state, with CO initially adsorbing on the perimeter of the perturbed surface region to produce a ring shaped pattern (Figure 7c). Figure 7d shows the final state of the surface, which at these conditions, is now completely CO-covered. Image intensity profiles, given in Figure 8, taken along the white line segment overlaid on Figure 7d, precisely show the location of the surface memory effect. The decreased image intensity values centered at 175 and 475 μm on the brightness profile taken at 140 s clearly show preferential CO adsorption taking place at the edges of the region previously occupied by the CO island at time zero in the sequence. This perimeter corresponds to the region of the surface where adsorbed CO was able to react with the O-adlayer. Based on this observation, it appears that reaction between adsorbates is a necessary step in the development of the surface memory effect. This claim is supported by the fact that a similar memory effect was observed following local H_2, NH_3, and O_2 perturbations to a monostable surface at temperatures ranging from 413 to 503 K, while perturbation of the surface with chemically inert gases, such as Ar and He, failed to induce any memory effect.

From the apparent dependence on the surface reaction and the spatial orientation of the memory effect, an explanation for the observed behavior could be based on a perimeter of clean, reconstructed hex surface remaining from the reaction between the doser-induced CO island and the O-adlayer. With the addition of CO globally to the gas-phase, CO could then selectively adsorb to these hex patches to form the ring pattern. This is unlikely though, as the memory effect has been observed after the surface has been exposed to 240,000 L of O_2, which is much greater than the minimum O_2 exposure of 600 L shown previously to lift the hex reconstruction.[15] Therefore, over the range of experimental conditions used to generate the memory effect, the entire surface should exist in a 1×1 configuration at the time of global CO addition to the reactor, with no localized hex heterogeneities present to cause the memory effect.

An annular shaped molecular stream, that is, a stream of higher molecular flux on the perimeter of the stream in relation to the center, produced by the capillary may also be eliminated as the source of the ring-shaped surface modification. Figure 9 shows a contour map and corresponding cross-

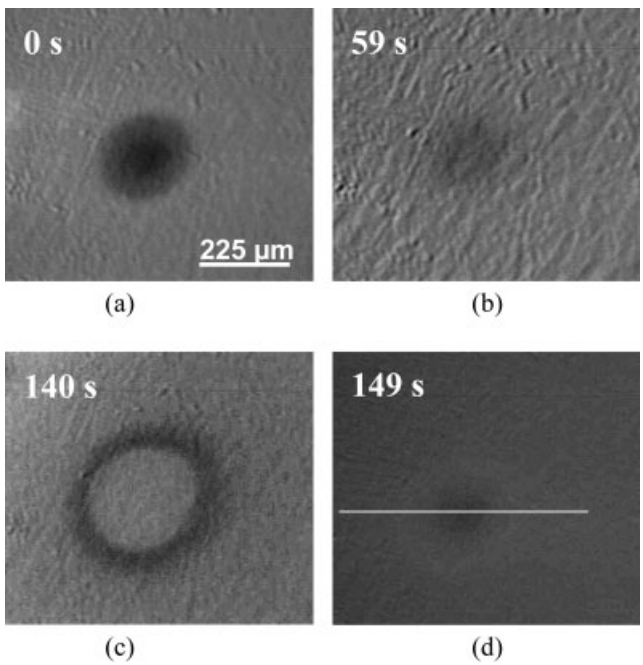

Figure 7. Illustration of memory effect due to local gas dosing.

(a) CO is locally dosed onto an oxygen saturated surface maintained at 413 K with $p_{O2} = 0.013$ Pa. After the doser is removed in (b), the affected surface returns to the O-covered state, with the exception of the center region, which still shows some signs of CO-poisoning, (c) shows the preferential adsorption of CO to the perimeter of the affected region, as the surface transitions to the CO-poisoned state, and (d) with the addition of 0.0013 Pa CO to the gas phase.

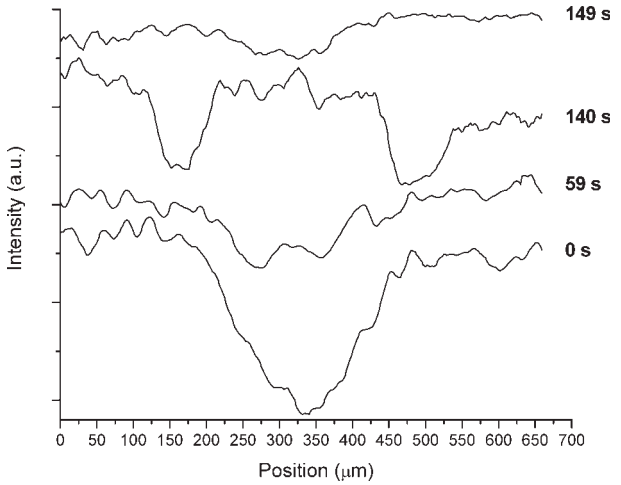

Figure 8. Brightness profile along line segment overlaid in Figure 7d at various time intervals.

The profiles show the location of the ring structure (140 s) in relation to doser-induced CO island (0 s) when CO was added globally to the reactor.

section of the relative gas flux within a He molecular stream emitted from a 30 μm capillary. The capillary was positioned at 400 μm from the sampling orifice to provide a spatially resolved approximation of the reactant flux experienced by the surface during a typical forcing experiment. As expected, the molecular flux through the orifice was highest at the center of the stream and decreased radially toward the edge of the stream. The profile proves the surface modification is not influenced by the geometry of the molecular stream emitted from the capillary, but rather a result of physicochemical process taking place on the catalytic surface once the local surface reaction is initiated. Such processes could include surface faceting[30,31] or the formation of a subsurface oxygen species at the CO/O reaction boundary previously identified at comparable reaction conditions using photoemission electron microscopy (PEEM).[32] In the case of local H_2 dosing, for example, it has been shown that the adsorption and desorption of H_2 produces long lasting defects on the surface.[26] Such defects may account for local differences in the adsorption probability of CO resulting in the creation of ring patterns and the CO islands mentioned previously.

If the surface is faceted or subsurface O is formed as a result of local gas dosing, it would be difficult to identify which structure in particular is causing the memory effect based entirely on the location of the selective CO adsorption alone. It is possible that either structure is produced along the CO/O reaction boundary. However, one distinguishing feature of the two structures is the temperature at which each can be removed from the surface. Falta et al. showed that by heating the surface to 500 K, any faceting or buckling of the Pt surface caused by a surface reaction is relaxed and the smooth surface is restored.[31] In contrast, if the memory effect were caused by a subsurface oxygen phase, the memory effect would remain intact well above temperatures approaching 500 K, on account that subsurface oxygen does not desorb from the surface until 720 K.[32] Additionally, CO is known to adsorb preferentially to Pt surface regions containing subsurface O relative to Pt-1 $\times$ 1 regions with O chemisorbed on the surface.[33] Therefore, if a subsurface O phase was formed at the reaction boundary between the doser-induced CO island and the O adlayer, it could result in the selective adsorption of CO in the ring geometry. Based on the difference in thermal stability between the two proposed structures, we performed experiments which probed the stability of the modified surface in order better understand the source of the observed memory effect. In these experiments, the modified surface was prepared using the local forcing procedure described previously, with one alteration. Following the removal of the local CO perturbation, but prior to global CO addition to the reactor, the surface was heated at a rate of 3 K/s in 0.013 Pa of O_2 to temperatures up to 588 K in an attempt to remove the memory effect from the surface. After the surface was cooled down the original

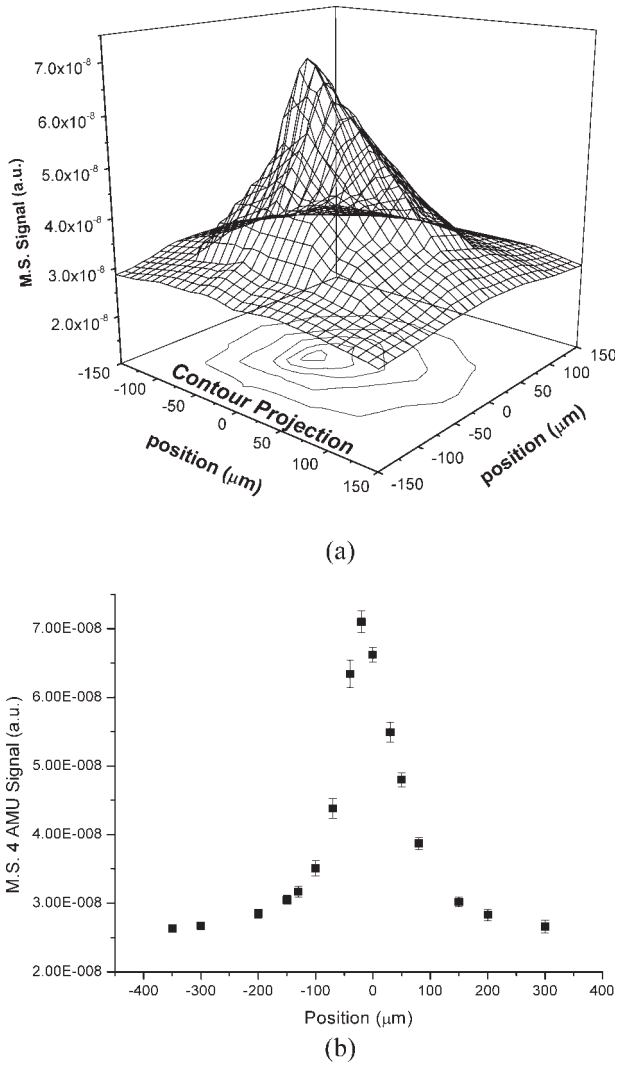

Figure 9. Profiles of molecular flux through a 10 μm orifice from a stream emitted from a 30 μm capillary.

(b) is a cross section of the contour plot in (a) taken at X = -25 μm. The plots show the 4 AMU mass spectrometer signal at various probe positions within the stream. He was the dosing gas, maintained at 120 Pa upstream of the capillary.

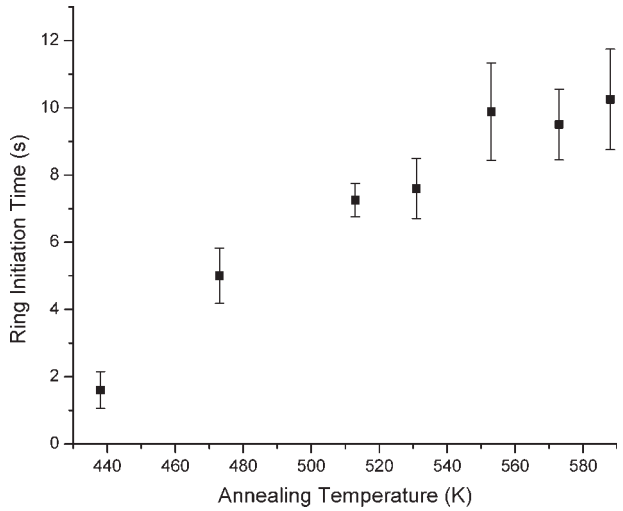

Figure 10. Ring initiation time for increasing surface annealing temperature.

Ring initiation time is defined as the time elapsed between local doser removal and global CO addition to the reactor. All ring patterns were created by dosing CO onto an O-covered surface at 438 K and 0.013 Pa global O_2. The doser was then removed and the surface was heated in 0.013 Pa O_2 at a rate of 3 K/s. The surface was allowed to cool to 438 K, where 0.0013 Pa CO was added globally to produce the ring formation.

forcing temperature of 438 K, 0.0013 Pa of CO was added globally to the reactor to initiate a ring pattern similar to that shown in Figure 7c. The time delay between global CO addition and the first observation of the adsorbed CO ring pattern, defined as the ring initiation time, was used as a relative measure of the extent to which the catalytic properties of the surface remained modified after surface heating. The effects of annealing on the surface memory effect are presented in Figure 10. The ring initiation time for a surface which was not annealed was found to be approximately 1.5 s. With increased annealing temperature, this value increased by up to a factor of five for a maximum annealing temperature of 588 K. The increase in ring initiation time is critical as it points out the thermal sensitivity of the modified surface. As the maximum annealing temperature increased, the longer times required to observe the ring pattern indicate that the properties of the modified surface are approaching those of the unforced surface. In other words, the memory effect is slowly being erased from the surface with increasing temperature. Also, the fact that preferential CO adsorption was observed after the surface was annealed to temperatures greater than 500 K suggests that surface faceting is not likely the cause of the memory effect. However, subsurface O remains a plausible source for the observed memory effect. While it has not been explicitly identified here, subsurface O cannot be disregarded as the source of the memory effect, given the relative stability and spatial arrangement of the surface memory identified through the selective adsorption of CO to the perturbed surface region.

Conclusions

The formation of locally confined oscillations and adsorbate islands are examples of novel complex behavior in surface reactions. These phenomena can only be observed when a nonlinear system, such as CO oxidation on Pt, is subjected to external forcing. The perturbation of the system allows access to the high-reactive rate branch at conditions where only a low-reactive state is typically observed, providing a potential pathway to the operation of catalysts in nonequilibrium regimes, with the prospective for novel and improved performance.

The creation of spatially confined adsorbate structures is attributed to a local modification of the catalytic surface properties due to external forcing. The properties of the modified surface have been systematically studied through the preferential adsorption of CO to surface regions subjected to local perturbation. Data regarding the modified surface suggests a thermally and temporally stable phase formed only in the presence of the surface reaction, such as subsurface O or a faceted surface. The geometric orientation, identified using EMSI, and the affinity of adsorbing species toward the modified surface region further suggest the possibility of a subsurface oxygen phase created at the forcing site. In order to discriminate between these two reaction-induced effects, modifications to the experimental setup are currently underway to incorporate PEEM to explicitly identify any subsurface oxygen species generated during the forcing process.

Acknowledgments

Acknowledgment is made to the donors of the American Chemical Society Petroleum Research Fund for support (or partial support) of this research and to W. Scott Neifert and Peter Welfel for assistance building the dosing equipment.

Literature Cited

1. Vanag VK, Epstein IR. Inwardly rotating spiral waves in a reaction-diffusion system. *Science*. 2001;294:835–837.
2. Toth A, Gaspar V, Showalter K. Signal transmission in chemical systems: propagation of chemical waves through capillary tubes. *J Phys Chem*. 1994;98:522–531.
3. Steinbock O, Muller SC. Chemical spiral rotation is controlled by light-induced artificial cores. *Physica A*. 1992;188:61–67.
4. Steinbock O, Zykov VS, Muller SC. Wave propagation in an excitable medium along a line of a velocity jump. *Phys Rev E*. 1993; 48:3295–3298.
5. Sakurai T, Mihaliuk E, Chirila F, Showalter K. Design and control of wave propagation patterns in excitable media. *Science*. 2002;296: 2009–2012.
6. Graham MD, Kevrekidis IG, Asakura K, Lauterbach J, Krischer K, Rotermund HH, Ertl G. Effects of boundaries on pattern formation: catalytic oxidation of CO on Pt. *Science*. 1994;264:80–82.
7. Wolff J, Papathanasiou AG, Kevrekidis IG, Rotermund HH, Ertl G. Spatiotemporal addressing of surface activity. *Science*. 2001;294: 134–137.
8. Lund CD, Surko CM, Maple MB, Yamamoto SY. Effects of local reactant concentration perturbations in oscillatory catalysis. *J Chem. Phys*. 1998;108:5565–5570.
9. Lund CD, Surko CM, Maple MB, Yamamoto SY. Effects of local reactant concentration perturbations in oscillatory catalysis. [Erratum to document cited in CA128:197230] *J Chem Phys*. 2000;112:1619.
10. Slin'ko MM, Jaegar NI. Oscillating Heterogeneous Catalytic Systems. In: Delmon B, Yates JT, editors. *Studies in Surface Science and Catalysis*. Amsterdam: Elsevier; 1994.
11. Imbihl R, Cox MP, Ertl G, Mueller H, Brenig W. Kinetic oscillations in the catalytic CO oxidation on Pt(100): theory. *J Chem Phys*. 1985;83:1578–1587.
12. Imbihl R, Cox MP, Ertl G. Kinetic oscillations in the catalytic CO oxidation on Pt(100): experiments. *J Chem Phys*. 1986;84:3519–3534.

13. Heinz K, Lang E, Strauss K, Muller K. Observation of the structural transition Pt(100) 1 × 1 to hex by LEED intensities. *Appl Surf Sci*. 1982;11/12:611–624.
14. Norton PR, Da Vies JA, Creber DK, Sitter CW, Jackman TE. The Pt(100) (5x20) to (1x1) phase transition: a study by Rutherford backscattering, nuclear microanalysis, LEED and thermal desorption spectroscopy. *Surf Sci*. 1981;108:205–224.
15. Barteau MA, Ko EI, Madix RJ. The adsorption of carbon monoxide, molecular oxygen, and molecular hydrogen on Pt(100)-(5x20). *Surf Sci*. 1981;102:99–117.
16. Barteau MA, Ko EI, Madix RJ. The oxidation of carbon monoxide on the Pt(100)-(5x20) surface. *Surf Sci*. 1981;104:161–180.
17. Hopkinson A, Guo XC, Bradley JM, King DA. A molecular beam study of the CO-induced surface phase transition on Pt(100). *J Chem Phys* 1993;99:8262–8279.
18. Morgan AE, Somorjai GA. Low energy electron diffraction studies of gas adsorption on the Pt(100) single crystal surface. *Surf Sci*. 1968;12:405–425.
19. Jackman TE, Griffiths K, Davies JA, Norton PR. Absolute coverages and hysteresis phenomena associated with the carbon monoxide-induced Pt(100) hex to (1x1) phase transition. *J Chem Phys*. 1983;79:3259–3533.
20. Behm RJ, Thiel PA, Norton PR, Ertl G. The interaction of carbon monoxide and Pt(100). I. Mechanism of adsorption and platinum phase transition. *J Chem Phys*. 1983;78:7437–7447.
21. Lele T, Lauterbach J. Spatio-temporal pattern formation during CO oxidation on Pt(100) at low and intermediate pressures: A comparative study. *Chaos*. 2002;12:164–171.
22. Lele T, Pletcher TD, Lauterbach J. Spatiotemporal patterns during CO oxidation on Pt(100) at elevated pressures. *AIChE J*. 2001;47: 1418–1424.
23. Rotermund HH, Haas G, Franz RU, Tromp RM, Ertl G. Imaging pattern formation in surface reactions from ultrahigh vacuum up to atmospheric pressures. *Science*. 1995;270:608–610.
24. Lauterbach J, Rotermund HH. Spatiotemporal pattern formation during the catalytic CO-oxidation on Pt(100). *Surf Sci*. 1994;311:231–246.
25. Fanson PT, Delgass WN, Lauterbach J. Island Formation during Kinetic Rate Oscillations in the Oxidation of CO over Pt/SiO_2: A Transient Fourier Transform Infrared Spectrometry Study. *J Catal*. 2001;204:35–52.
26. Dixon-Warren SJ, Pasteur AT, King DA. Nonlinear effects in the hydrogen/deuterium catalytic exchange reaction over Pt(100). *J Chem Phys*. 1995;103:2261–2271.
27. Gorodetskii VV, Matveev AV, Cobden PB, Nieuwenhuys BE. Study of H_2, O_2, CO adsorption and $CO+O_2$ reaction on Pt(100), Pd(110) monocrystal surfaces. *J Mol Catal A: Chemical*. 2000;158:155–160.
28. Lombardo SJ, Fink T, Imbihl R. Simulations of the nitric oxide + ammonia and nitric oxide + hydrogen reactions on Pt(100): steady-state and oscillatory kinetics. *J Chem Phys*. 1993;98:5526–5539.
29. Lu KE, Rye RR. Flash desorption and equilibrium of molecular hydrogen and molecular deuterium on single crystal surfaces of platinum. *Surf Sci*. 1974;45:677–695.
30. Uchida Y, Lehmpfuhl G, Imbihl R. Reflection electron microscopy of the catalytic etching of platinum single-crystal spheres in carbon monoxide and oxygen. *Surf Sci*. 1990;234:27–36.
31. Falta J, Imbihl R, Sander M, Henzler M. Low-energy electron-diffraction profile analysis of reaction-induced substrate changes on Pt(110) during catalytic CO oxidation. *Phys Rev B*. 1992;45:6858–6867.
32. Rotermund HH, Lauterbach J, Haas G. The formation of subsurface oxygen on Pt(100). *App Phys. A: Solids and Surfaces* 1993;A57: 507–511.
33. Lauterbach J, Asakura K, Rotermund HH. Subsurface oxygen on Pt(100): kinetics of the transition from chemisorbed to subsurface state and its reaction with CO, H_2 and O_2. *Surf Sci*. 1994;313:52–63.

Manuscript received Apr. 15, 2008, and revision received July 30, 2008.